Tectonophysics 608 (2013) 914–928

Contents lists available at ScienceDirect

Tectonophysics

journal homepage: www.elsevier.com/locate/tecto

Analyzing the drainage system anomaly of Zagros basins: Implications for active tectonics

Shahram Bahrami *

Department of Physical Geography, Faculty of Geography and Environmental Science, Hakim Sabzevari University, Sabzevar, Iran

ARTICLE INFO

Article history:
Received 1 March 2013
Received in revised form 22 June 2013
Accepted 20 July 2013
Available online 31 July 2013

Keywords:
Hierarchical anomaly number
Basin shape
Hinge spacing
Zagros
Tectonic

ABSTRACT

Morphometric analysis of hierarchical arrangement of drainage networks allows to evaluate the effects of external controls especially tectonics on basin development. In this study, a quantitative method for calculation of stream's hierarchical anomaly number is introduced. Morphometric parameters such as hierarchal anomaly index (Δa), percent of asymmetry factor (PAF), basin Shape (Bs), basin length to mean width ratio (Bl/Bmw), stream's bifurcation ratio (Rb), bifurcation index (R), drainage density (Dd), drainage frequency (Df) and anticline's hinge spacing (Hs) of 15 basins in Zagros Mountains were examined. Results show that the strong correlations exist between pairs Δa–PAF ($r = 0.844$), Δa–Bs ($r = 0.732$), Δa–Bl/Bmw ($r = 0.775$), Δa–R ($r = 0.517$), PAF–Bl/Bmw ($r = 0.519$), Bs–R ($r = 0.659$), Bl/Bmw–R ($r = 0.703$), Hs–Δa ($r = -0.708$), Hs–PAF ($r = -0.529$) and Hs–Bs ($r = -0.516$). The variations in trend of anticlines control the shape of basins so that where anticlines hinges become closer to each other in the downstream direction, basin become narrower downward and hence the Δa increases. The more uplifted northeastern anticlines cause the trunk river of the basins to migrate toward the younger anticlines in southwest and hence Δa increases because the trunk river receives a lot of first order streams. Data reveal that the rate of Δa is higher in elongated synclinal basins. Due to the decrease in the intensity of deformation from northeast toward southwest of Zagros, the hinge spacing of anticlines increases southwestwards. Data reveal that the variation in hinge spacing of anticlines strongly controls the basin's shape and tilting as well as the hierarchical anomaly of drainage system. Since the elongation and tilting of basins are associated with the variations in rates of folding, uplift and hinge spacing of anticlines, it can be concluded that the hierarchical anomaly of drainages in studied basins is controlled by the intensity of Zagros tectonic activities.

1. Introduction

Rivers and their tributaries are the key features of a drainage basin. The quantitative study of drainage system was initiated by Horton (1945) followed by Strahler (1952), in which they introduced the concept of stream ordering. Morphometric characteristics of drainage system of many basins and sub basins in different parts of the globe have been studied widely (Abrahams, 1984; Altin and Altin, 2011; Horton, 1945; Krishnamurthy et al., 1996; Kumar et al., 2000; Leopold and Miller, 1956; Reddy et al., 2004; Shreve, 1966; Strahler, 1952, 1957).

The development of landscapes in tectonically active areas results from a complex integration of the effects of vertical and horizontal motions of crustal rocks and erosional processes (Burbank and Anderson, 2001). In tectonically active regions especially in folded mountains, qualitative and quantitative analyses of drainage systems are useful to evaluate the impact of tectonic activity on geomorphic processes and landscape development (Burbank and Anderson, 2001; Delcaillau et al., 1998; Delcaillau et al., 2006; Jackson et al., 1998; Ramsey et al., 2008; Sung and Chen, 2004).

Morphometric parameters of drainage system such as drainage density and frequency, bifurcation ratio, confluence angle have been widely analyzed in relation to active tectonics (Deffontaines and Chorowicz, 1991; Devi et al., 2011; Jamieson et al., 2004; Simoni et al., 2003; Talling and Sowter, 1999; Zhang et al., 2006).

The analysis of drainage pattern and anomaly also has the potential to record evidence of active tectonic and fold growth (Deffontaines et al., 1992; Delcaillau et al., 2006; Ramasamy et al., 2011; Simoni et al., 2003).

Most recently, some researchers have introduced valuable attributes of drainage systems and their relevance to active tectonics. For example, Ramsey et al. (2008) revealed that the development of distinctive asymmetric forked tributary patterns and the curve of the tributary headwaters into a direction parallel to the fold crest are geomorphic evidence of lateral fold growth in Zagros, Iran.

Bretis et al. (2011) demonstrated that the development of asymmetric forked drainage network and curved wind gaps are powerful geomorphic indicators showing lateral propagation of Bana Bawi, Permam and Safeen anticlines in NE Iraq.

* Tel.: +98 5714003231; fax: +98 5714003270.
E-mail addresses: s.bahrami@hsu.ac.ir, shahram_bahrami2003@yahoo.com.

0040-1951/$ – see front matter © 2013 Elsevier B.V. All rights reserved.
http://dx.doi.org/10.1016/j.tecto.2013.07.026

Ramasamy et al. (2011) mapped some drainage anomalies like deflected drainages, eyed drainages and compressed meanders of South India and, thereby, detected a series of faults with well-defined morphology. Based on the interpretation of drainage anomalies and the related lineaments/faults, they have provided definite information for the post collision tectonics, which are currently active, and hence bear greater significance in the context of fast relapsing seismicities in the area.

Walker and Allen (2012) revealed that right-lateral movement of the Kuh Banan Fault in eastern Iran has resulted in the formation of numerous river offsets. They noted that small and highly variable drainage spacing ratios of the Kuh Banan fault is due to structural complexity and resultant topographic variation deflecting rivers and affecting drainage basin shapes on smaller scales.

Based on the qualitative and quantitative geomorphic analyses, Giaconia et al. (2012) showed that the reverse faults of Cabrera, SE Spain, have produced knickpoints, stream deflections, complex basin hypsometric curves, high SLk (normalized stream-length gradient index) anomalies and highly eroded basins in their proximity. They also revealed that the drainage network shows an S-shaped pattern reflecting progressive anticlockwise rotation related to the sinistral Palomares fault zone.

Based on parameters of the hierarchy of the drainage network such as bifurcation ratio (Rb) and bifurcation index (R), Raj (2012) noted that the eastward tilting of the drainage systems in the NE Gujarat (India) and the movement along various faults in the region has resulted in the poor organization of some hydrographic networks.

Although drainage system characteristics and tectonic interactions have been widely studied, little work is available on the hierarchical arrangement of drainage systems. The hierarchical organization of drainage networks has first been analyzed by means of bifurcation ratio (Horton, 1945). Subsequently, in order to better define the organization of drainage system, Avena et al. (1967) introduced the direct bifurcation ratio (Rbd), bifurcation index (R), hierarchical anomaly number (Ha), hierarchical anomaly index (Δa) and hierarchical anomaly density. Some researchers have evaluated the application of hierarchical anomaly number (Ha) and index (Δa) to detect tectonic activity (Guarnieri and Pirrotta, 2008) and to estimate the suspended sediment yield of basins (Ciccacci et al., 1986; Della Seta et al., 2009; Della et al., 2007; Gioia et al., 2011; Grauso et al., 2008).

Guarnieri and Pirrotta's (2008) studies on the Ha and Δa parameters showed the limited organization of the drainage system of the Curcuraci and Papardo fiumare basin (in the Sicilian side of the Messina Strait, NE Sicily) due to active tectonics.

Tectonically active and young Zagros Folded belt (Berberian, 1995) is composed of NW–SE trending and whaleback anticlines and synclines with large variation of fold dimensions. Although some researchers (Alipoor et al., 2011, 2012; Bahrami, 2012; Bretis et al., 2011; Piraste et al., 2011; Ramsey et al., 2008) have analyzed the relations between active tectonics and drainage systems, the quantitative evaluation of hierarchical arrangement of drainage systems in Zagros in currently lacking.

The aim of this research is to introduce a quantitative method for the calculation of hierarchical anomaly number in every drainage junction (path) and thereby in the whole catchment. In this study, 15 catchments with different shapes and areas in the Folded Zagros were selected, then hierarchical anomaly index (Δa) of streams were calculated, and results were correlated with other morphometric indexes of catchments.

2. Study area

Studied basins in SW Iran (Fig. 1) lie within the Zagros Simply fold belt. A total of 15 basins were selected in 3 provinces. Basins 1 to 6 are located in Kermanshah, basins 7, 8, 9, 11 and 12 are parts of Ilam and basins 10, 13, 14 and 15 are located in Lorestan province.

Structurally, the studied basins are part of the Zagros belt in southwest Iran. Zagros belt as a part of Arabia–Eurasia collision zone extends for 1500 km from the Taurus Mountains in southeast Turkey through southwest Iran, and terminates near the Hormuz Strait at the mouth of the Persian Gulf. Geomorphologically, Zagros belt is divided into two adjacent belts: the High Zagros Belt and the Zagros Simply Folded Belt (ZSFB), separated by the High Zagros Fault (Berberian and King, 1981; Falcon, 1974). The ZSFB is bounded to the northeast by the Zagros Main Thrust and separated by this fault from the Sanandaj–Sirjan metamorphic belt (Emami, 2008).

The ZSFB results from the closure of the Neo-Tethys Ocean between the Arabia margin and the Eurasia continent (Stocklin, 1968).

Since the onset of continent–continent collision between the Arabian and Iranian plates in the Tertiary, a major pulse of compressional deformation has been propagating southwestward, away from the collision zone and towards the foreland (Sepehr et al., 2006). The GPS measurements indicate that shortening is not distributed homogeneously either along or across the Zagros belt (Hessami et al., 2006).

Falcon (1974) inferred that the regional uplift represented by 'geo-flexure' implied that the Zagros had risen at a minimum rate of 1 mm/yr since the early Pliocene.

According to Tatar et al. (2002), present-day NE–SW shortening across the central part of the Simple Folded Zone of Zagros is c. 10 mm/yr. Blanc et al. (2003) suggested that, if the Simple Folded Zone deformation has taken place since c. 5 Ma, this corresponds to a shortening rate of c. 10 mm/yr which is a substantial part of the present Arabia–Eurasia convergence rate. Based on a few stations located in the Zagros, Nilforoushan et al. (2003) and Vernant et al. (2004) showed that the rate of shortening increases from 4 ± 2 mm/yr in the NW to 9 ± 2 mm/yr in the SE Zagros. Generally, rates of deformation and shortening diminish southwestwards in the Zagros fold–thrust belt (Hessami et al., 2006; Lawa et al., 2013).

The stratigraphy of the NW Zagros is a 10–12 km-thick section of lower Cambrian through Pliocene strata (Falcon, 1969). The stratigraphic column of Zagros is divided into the five structural divisions (Colman-Sadd, 1978); the Basement group, the Lower Mobile group, the Competent group, the Upper Mobile group and the Incompetent group (for stratigraphic details of Zagros, see Colman-Sadd, 1978; Alavi, 2004).

The lithological units outcropping in the studied basins are Sarvak (Limestone and shale), Gurpi (marl and marly limestone), Pabdeh (calcareous shale, marl and mudstone), Amiran (conglomerate, sandstone, siltstone and shale), Taleh Zang (limestone with intercalations of shale and argillaceous limestone), Kashkan (siltstone, sandstone and conglomerate), Asmari (limestone and dolomitic limestone), Gachsaran (marl and limestone with intercalations of gypsum and anhydrite), Mishan (marl and limestone), Agha jari (marl and sandstone), Bakhtiari (conglomerate) and Quaternary Alluviums. The area percent of lithological units for all basins is given in Table 1.

The ZSFB is composed of long, asymmetrical, whaleback or box-shaped anticlines which generally trend NW–SE. According to Colman-Sadd (1978), most folds in the simply folded belt of Zagros are asymmetric and, with a few exceptions, the steepest limbs of the anticlines are on the southwestern limbs. Narrow and V-shaped valleys are characteristics of the steep slopes of anticlines (Fig. 2e). Since the majority of anticlines around studied basins are composed of carbonate rocks (i.e. Asmari unit), karstic features are dominant landforms of the study area (Fig. 2a). The most typical karstic features of basins are karrens, dolines, and caves.

The area, perimeter and topographic characteristics of basins are given in Table 2. The lowest value of area is related to basin 11 (10.75 km^2) and the highest value is associated with basin 4 (285 km^2). The maximum elevation is related to basin 8 (2620 m a.s.l) and the minimum elevation is associated with basin 12 (510 m). The mean elevation is higher in basins 5, 6 and 9 than other basins. The value of mean slope is higher in basins 12, 13 and 14 (respectively 40.56%, 37.93% and 31.7%) than other ones (Table 2).

Hydrologically, basins 1 to 4 are upstream sub-basins of Alvand River that flows to Iraq near the town of Qasre-Shirin. Basins 5, 6, 8 and 10 to

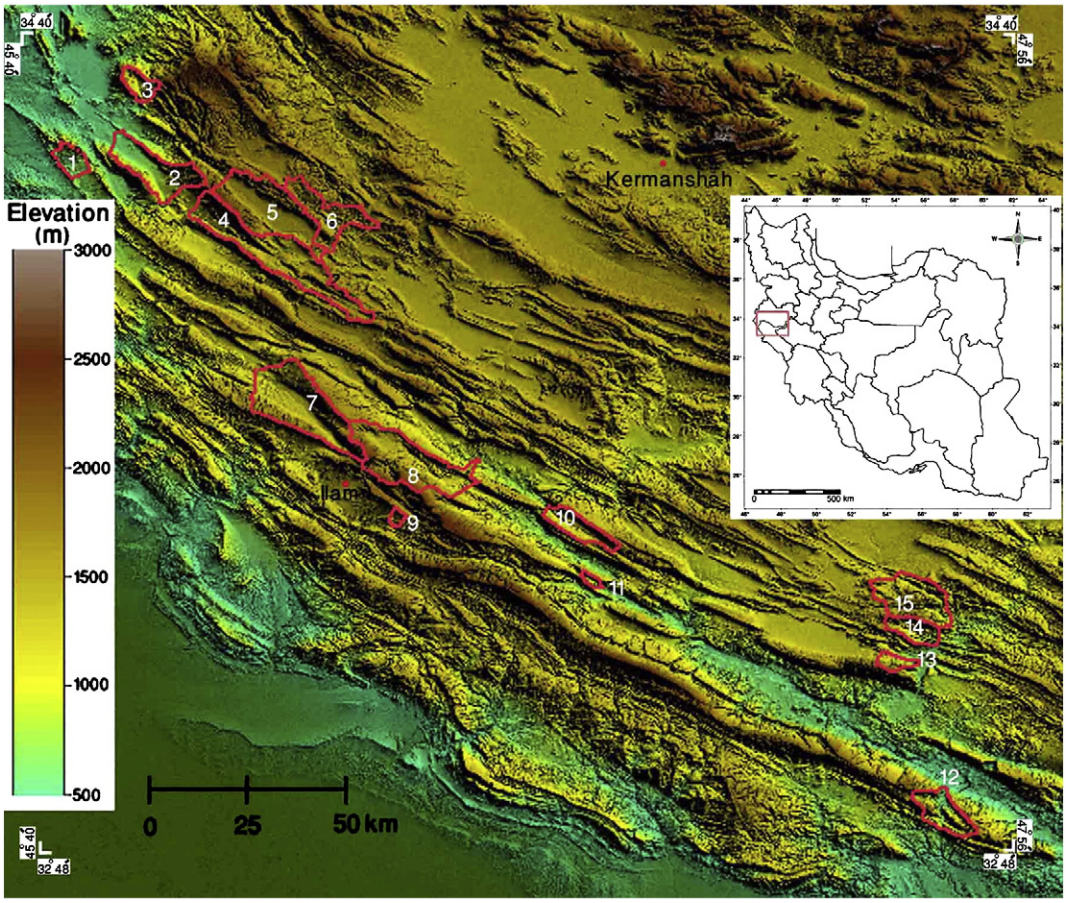

Fig. 1. Location map and SRTM DEM of studied basins in the Zagros Folded belt. Red lines show the basins borders.

15 are upstream sub-basins of Kashkan River entering Persian Gulf. Basin 7 is a sub-basin of Kangir River and basin 9 is a sub-basin of Konjancham River entering Iraq.

3. Materials

For quantitative evaluation of the drainage system hierarchical anomalies and their relevance to tectonic activity, 15 basins were selected in the simply folded belt of Zagros Mountains. The borders of basins were delineated from 1:50,000 topographic maps of Iranian National Geography Organization. Digital Elevation Models (DEMs) were prepared using ILWIS (Integrated Land and Water Information System) software after digitizing 20-m contour lines. After digitizing basins boundaries, the areas, perimeters, lengths and widths of basins were obtained. The maximum, minimum and mean elevations for every basin were obtained from DEMs. Slope map of basins were prepared in ILWIS software and the mean slope of each basin was calculated from all pixels of slope map.

After digitizing streams of basins (Figs. 3 and 4), the stream orders were assigned following Strahler's ordering system (Strahler, 1957). Then, stream length and number for each order were calculated. The stream junctions or paths (i → j) were identified and subsequently the number of streams in each junction ($Ns_{i \to j}$) was obtained. Geological units and their areas were derived from 1:250,000-scale geological maps of National Iranian Oil Company.

In order to study the effect of tectonic activity on drainage system and basins morphometry, at first, hinges or axial traces of anticlines were delineated based on 1:250,000-scale geological maps. Then the

Table 1
Area percent of geological units in studied basins.

Geological formations	1	2	3	4	5	6	7	8	9	10	11	12	13	14	15
Quaternary alluvium	0.0	41	0	30	43.1	8.1	23.9	15.9	32.3	9.8	0	14.3	21.3	14.6	14.4
Bakhtiari	0.0	0	0	0.3	0.1	0	0	0.2	0	0	0	0	0	0	0
Agha Jari	0.0	4.7	0	0	1.1	0	0	0.8	0	0	0	0	0	0	0
Mishan	0.0	0.4	0	0	0	0	0	0	0	0	0	0	0	0	0
Gachsaran	0.0	0	34	0.6	0	0	7.9	14.3	0	28.2	55.4	2.7	11.8	2.3	13.6
Asmari	1.0	44.3	66	69.2	53.3	91.9	68.2	58.8	55.8	62	44.6	15	51.3	28.8	40.1
Kashkan	0.0	0	0	0	0.1	0	0	0	0	0	0	0	15.6	12.7	28.1
Taleh Zang	12.6	9.6	0	0	1.4	0	0	0	0	0	0	0	0	11.4	3.8
Amiran	65.3	0	0	0	0.9	0	0	0	0	0	0	0	0	30.2	0
Pabdeh	0.0	0	0	0	0	0	0	7.3	11.9	0	0	20.1	0	0	0
Gurpi	21.1	0	0	0	0	0	0	2.7	0	0	0	7	0	0	0
Sarvak	0	0	0	0	0	0	0	0	0	0	0	40.9	0	0	0
Sum	100	100	100	100	100	100	100	100	100	100	100	100	100	100	100

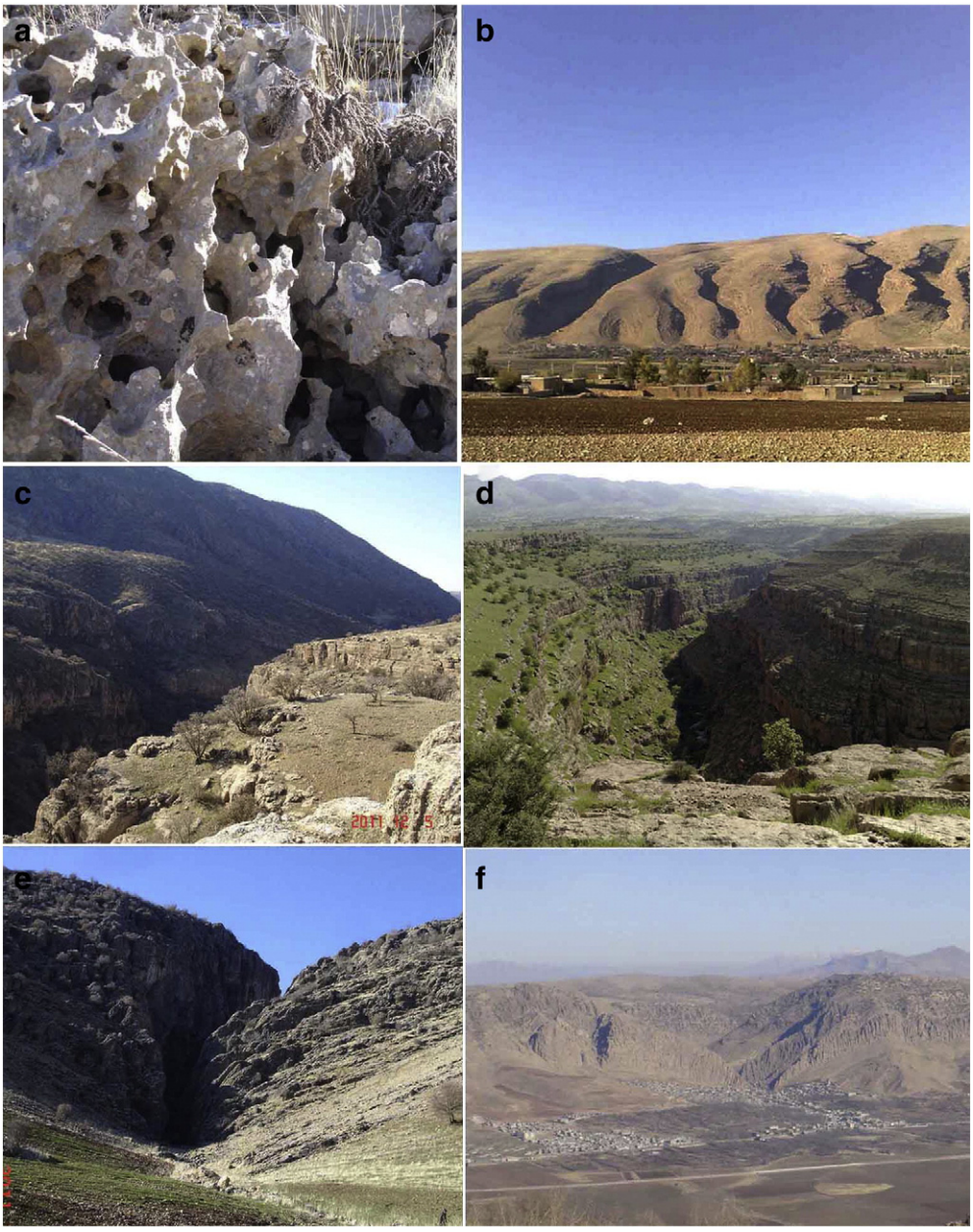

Fig. 2. Photographs of some landforms of study area: (a) karrens developed on karstic rocks of Asmari formation in basin 5; (b) an example of parallel, first/second order streams entrenched into the karstic limb of Danehkhoshk anticline in southwest of basin 2; (c) deeply entrenched Paykola river in the southeast of Paykola anticline, in the southwest of basin 4; (d) deeply incised and meandering Golin river in the south east of Denehkhoshk anticline, in the southeastern end of basin 2; (e) narrow and V-shaped valleys formed on the steep slope of Noakoh anticline in the southwest of basin 5; (f) typical water gap formed on the Kerend anticline in the northeast of basin 5.

hinge spacing (Hs) of anticlines around studied basins were measured. The Hs index for every basin was measured at five lines perpendicular to anticline hinges.

Several field trips were carried out to identify landforms and processes of basins.

4. Morphometric indexes

4.1. Drainage system morphometry

4.1.1. Hierarchical anomaly number

The drainage system of a basin is subdivided into fluvial segments of increasing hierarchical order (Horton, 1945). In the Strahler ordering system (Strahler, 1957), all headwater tributaries (nearest the basin divide) are referred to as first-order streams. Two first order streams then produce a second order stream, two second order stream provide a third order, and so forth. The number of stream junctions of basins increases with increasing the stream order at the outlet of basins. For example, a basin with the highest stream order of 4 has 6 stream junctions ($1 \rightarrow 2$, $1 \rightarrow 3$, $1 \rightarrow 4$, $2 \rightarrow 3$, $2 \rightarrow 4$ and $3 \rightarrow 4$ junctions) whereas a basin with the highest stream order of 5 has 10 stream junctions ($1 \rightarrow 2$, $1 \rightarrow 3$, $1 \rightarrow 4$, $1 \rightarrow 5$, $2 \rightarrow 3$, $2 \rightarrow 4$, $2 \rightarrow 5$, $3 \rightarrow 4$, $3 \rightarrow 5$ and $4 \rightarrow 5$ junctions). Some stream junctions have hierarchical organization (i.e. $1 \rightarrow 2$, $2 \rightarrow 3$ and $3 \rightarrow 4$ junctions) whereas some stream junctions have hierarchical anomalies (i.e. $1 \rightarrow 3$, $1 \rightarrow 4$, $2 \rightarrow 4$ junctions). Overall, streams of i-order that flow in streams of $i + 2$, $i + 3$ and etc. orders, are anomalous stream junctions.

Avena et al. (1967) defined the hierarchical anomaly number (Ha) as the minimum number of first-order segments necessary to render the network perfectly hierarchical (Guarnieri and Pirrotta, 2008). The drawback of the Avena et al. (1967) method is the manual calculation of Ha parameter. In this study, equations are introduced for the

Table 2
The area (km^2), perimeter (km), maximum height (m), minimum height (m), means height (m) and mean slope (%) of studied basins.

Basin no.	Area	Perimeter (km)	H maximum (m)	H min (m)	H mean (m)	Mean slope%
1	40.76	28.74	1120	580	756	13.22
2	147.1	65.25	2280	590	1296	25.71
3	56.48	34.22	2110	655	1208	26.48
4	285	121.8	2460	980	1517	21.4
5	237.7	81.96	2460	1410	1678	17.26
6	124	77.15	2020	1380	1628	16.85
7	273.5	85.09	2610	1049	1486	18.48
8	249.8	93.13	2620	848	1530	22.63
9	10.86	13.79	1985	1396	1616	24.6
10	69.78	47.26	1830	790	1357	24.99
11	10.75	15.18	1410	718	1090	29
12	88.44	47.46	1990	510	1081	40.56
13	24.51	25.38	1990	717	1256	37.93
14	56.27	34.33	1830	720	1189	31.6
15	150.7	57.87	1830	830	1332	26.64

calculation of hierarchical anomaly number for every stream junction ($Ha_{i\to j}$) and hierarchical anomaly number of the whole basin (Ha_t). The $Ha_{i\to j}$ is calculated based on following Eq. (1):

$$Ha_{i\to j} = 2^{(j-2)} - 2^{(i-1)}. \quad (1)$$

The higher the difference between *i* and *j*, the higher the hierarchical anomaly number (column 2 in Table 3). After calculation of $Ha_{i\to j}$, the number of streams for each junction ($Ns_{i\to j}$) of basin was obtained. The hierarchical anomaly number of the whole catchment (Ha_t) is calculated from the sum of $Ha_{i\to j}$ multiplied by $Ns_{i\to j}$:

$$Ha_t = \sum\left(Ha_{i\to j} \times Ns_{i\to j}\right). \quad (2)$$

4.1.2. Hierarchical anomaly index (Δa)

The Δa index is calculated from Ha_t divided by the actual number of first-order streams (N_1):

$$\Delta a = Ha_t / N_1. \quad (3)$$

Fig. 5 shows the procedure for the calculation of $Ha_{i\to j}$, Ha_t and Δa parameters in a conceptual basin. The Δa parameter is highly sensitive to the effects of tectonic activity (Guarnieri and Pirrotta, 2008). In tectonically active mountains such as Zagros that basins are elongated due to the effect of long anticlines and synclines, the value of Ha_t index seems to be high in comparison with the N_1 parameter and hence the Δa values of basins are high.

4.1.3. Bifurcation index (R)

The R index is the difference between the bifurcation ratio (Rb) and the direct bifurcation ratio (Rbd). The Rb for a given order (i) is defined as the number of streams of i order divided by the number of streams of order i + 1(Horton, 1945; Strahler, 1952). The Rbd for a given (i) order is the number of streams of order i that flow in streams of next, higher order (i + 1) divided by the number of streams of order i + 1. The R index depends on the presence of hierarchical anomalies in the network and can give useful information on the typology of the active erosive processes and on the degree of evolution of a basin (Guarnieri and Pirrotta, 2008).

4.1.4. Drainage frequency and density

Drainage density (Dd) is an important morphometric index for channel networks that reflects the processes governing landscape dissection (Schumm, 1997). This parameter may provide clues to reveal the effect of active tectonics (Devi et al., 2011; Han et al., 2003; Talling and Sowter, 1999). Drainage density is defined as total stream length per unit area of a river basin. Drainage frequency (Df) is the total number of stream segments of all orders per unit area (Horton, 1932). The high stream frequency is usually related to impermeable rocks, sparse vegetation, high relief conditions and low infiltration capacity (Ozdemir and Bird, 2009; Shaban et al., 2005). The value of drainage density and frequency can be useful criteria in evaluating the rates of uplift and lateral propagation of anticlines (Keller and Pinter, 2002; Keller et al., 1999; Melosh and Keller, 2013).

4.2. Basin morphometry

4.2.1. Percent of basin asymmetry (PAF)

Asymmetry factor (Af) is one of the ways to evaluate the existence of tectonic tilting at the scale of a drainage basin (El Hamdouni et al., 2008; Keller and Pinter, 2002; Ozkaymak and Sozbilir, 2012). The Af is defined as; $Af = 100(A_r/A_t)$, where A_r is the drainage area on the right hand (facing downstream) of the trunk stream and A_t is the total area of the drainage basin. Values of Af significantly greater or less than 50 may suggest tilting. When Af is greater than 50, the main channel has shifted towards the left side of the basin (tilting of basin towards the left). A value less than 50 indicates that the main channel has shifted towards the right side of the basin (tilting of basin towards the right).

In this study, Af index has been revised as the percent of asymmetry factor (PAF):PAF = (ALS/At) 100, where ALS is the area of larger side of the trunk stream of basin and At is the total area of the basin. The PAF value of close to 50 shows that there is no (or little) tilting of basins. The PAF value does not show the tilting of basins towards right or left side. It only reveals the percent or degree of tilting of basins. Values of PAF significantly greater than 50 (close to 100) suggest the high percent of basin asymmetry.

4.2.2. Basin shape parameters

The horizontal projection of a basin may be described by the basin shape index or the elongation ratio, Bs (Cannon, 1976; Ramírez-Herrera, 1998), expressed by:

$$\mathrm{Bs} = \mathrm{Bl}/\mathrm{Bw} \quad (4)$$

where Bl is the length of the basin, measured from its mouth to the most distant drainage divide, and Bw is the width of a basin measured at its widest point.

Relatively young drainage basins in active tectonic areas tend to be elongated in shape, normal to the topographic slope of a mountain (Bull and McFadden, 1977; El Hamdouni et al., 2008; Faghih et al., 2012; Ramírez-Herrera, 1998). Basin shapes become progressively more circular with time after cessation of mountain uplift. In tectonically active mountain fronts such as Zagros Folded Belt, the value of Bs tends to be high due to the elongated basins located between long uplifting anticlines.

Due to the variation of Zagros folds length and wavelength (Burberry et al., 2010; Casciello et al., 2009) the width of basins varies greatly within Zagros Mountains. It seems that the Bw cannot be an appropriate representative of basins width in Zagros Mountains. Therefore, the basin length to mean width ratio (Bl/Bmw) was also calculated in this study. The Bmw is the mean of basin width measured in this study at 10 lines perpendicular to the basin length.

5. Results

Figs. 3 and 5 show the drainage map of studied basins. There is considerable variation in drainage pattern among basins. In most basins especially long ones, trunk streams follow the syncline hinge orientated NW–SE, while most drainages are mainly oriented perpendicular to the fold hinge. Dendritic drainage pattern is observed in circular and wider basins (i.e. 1, 3, 7, 9, 12 and 15). Long and narrow basins consist of

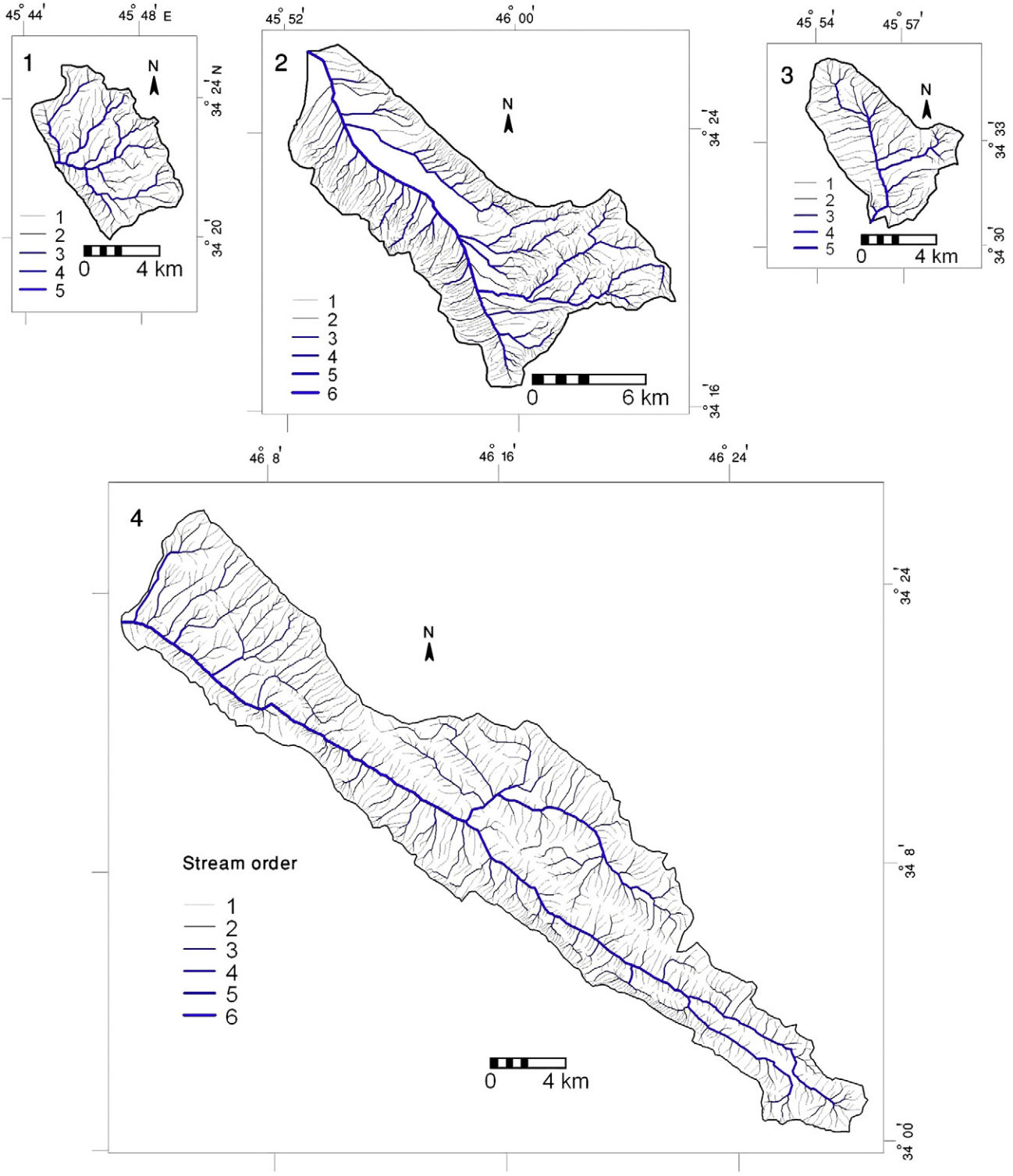

Fig. 3. Drainage map of basins 1 to 4. The hydrographic network is represented according to Strahler's ordering system.

parallel streams (Fig. 2b). Trellis and dendritic drainage network are observed in basins 2, 4, 5 and 8. Apart from drainage pattern variations among basins, considerable variations in channel pattern are observed in every basin. For example, dendritic, trellis and parallel patterns are developed in basin 5 in which dendritic and trellis patterns are associated with wide upstream areas whereas parallel pattern is related to narrow downstream parts (Fig. 4).

The values of Ha_t and Δa indexes are given in Table 3. The Ha_t values of basins range from 40 (basin 9) to 3057 (basin 4). Table 3 shows that, in basins with higher Ha_t values, the number of streams with low order (i.e. 1) joining to higher order (i.e. 5 or 6) is considerably higher. For example, in basins 4 and 7 with same area, the number of 1st order streams joining the 5th order streams ($Ns_{1\rightarrow 5}$) is 89 in basin 4 (with higher Ha_t) while it is 19 in basin 7 (with lower Ha_t).

The values of hierarchical anomaly index (Δa) of basins vary from 0.64 (basin 1) to 3.4 (basin 4). The values of the percent of asymmetry factor of basin (PAF), basin shape (Bs), the basin length to mean width ratio (Bl/Bmw), bifurcation index (R), bifurcation ratio (Rb), drainage

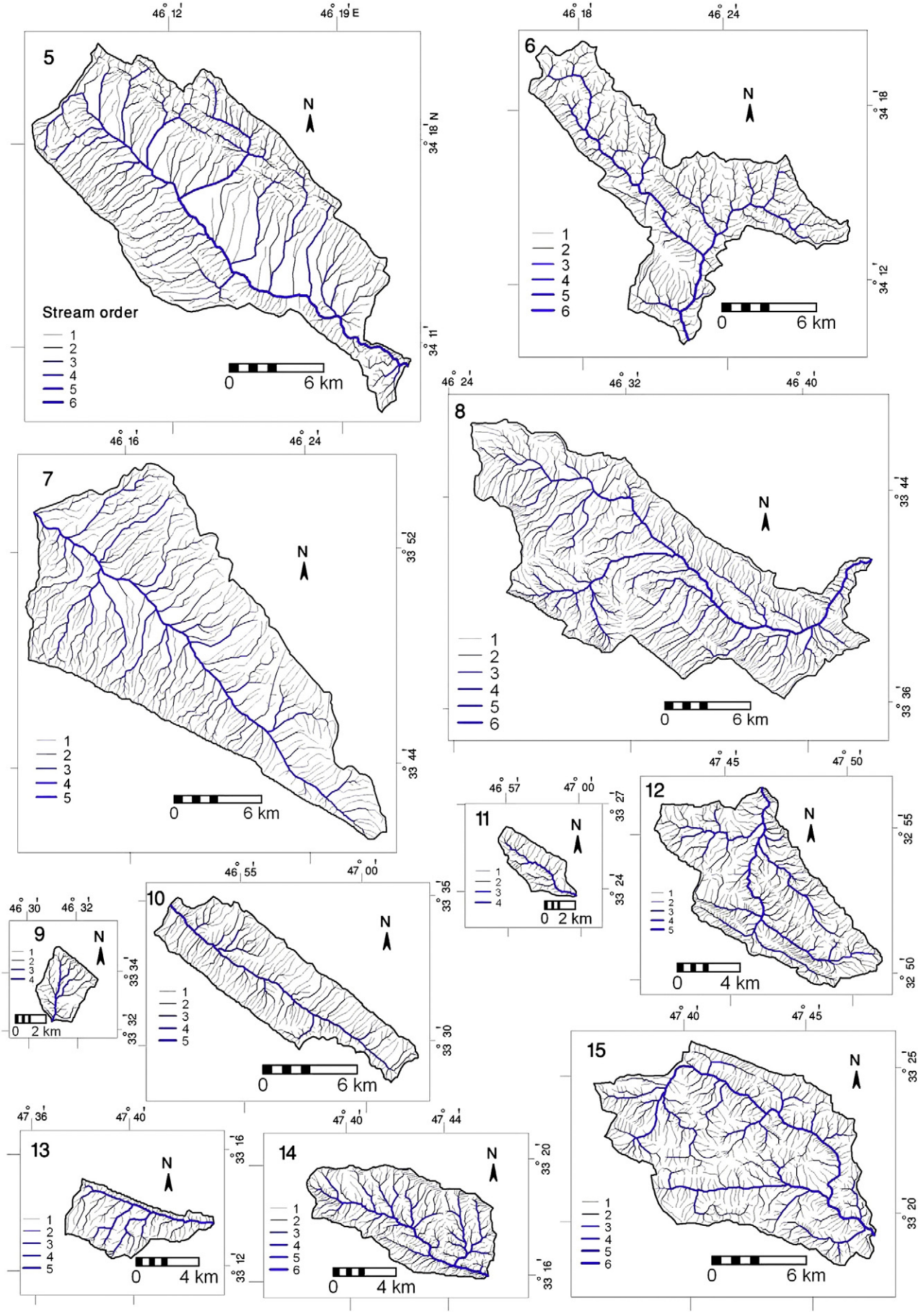

Fig. 4. Drainage map of basins 5 to 15. The hydrographic network is represented according to Strahler's ordering system.

Table 3
Stream junctions (i → j), hierarchical anomaly number of every stream junction ($Ha_{i\to j}$), number of streams for each junction ($Ns_{i\to j}$), $Ha_{t\to j}$ by $Ns_{i\to j}$, hierarchical anomaly number of the whole basin (Ha_t) and hierarchal anomaly index (Δa) in studied basins.

i → j	A ($Ha_{i\to j}$)	Basin 1 B ($Ns_{i\to j}$)	Basin 1 A×B	Basin 2 B	Basin 2 A×B	Basin 3 B	Basin 3 A×B	Basin 4 B	Basin 4 A×B	Basin 5 B	Basin 5 A×B	Basin 6 B	Basin 6 A×B	Basin 7 B	Basin 7 A×B	A	B	Basin 8 A×B	Basin 8 B	Basin 9 A×B	Basin 9 B	Basin 10 A×B	Basin 10 B	Basin 11 A×B	Basin 11 B	Basin 12 A×B	Basin 13 B	Basin 13 A×B	Basin 14 B	Basin 14 A×B	Basin 15 B	Basin 15 A×B
1 → 2	0	141	0	391	0	100	0	555	0	405	0	376	0	363	0	0	637	0	42	0	144	0	35	0	316	0	63	0	246	0	446	0
1 → 3	1	19	19	96	96	12	12	94	94	103	103	51	51	47	47	1	108	108	3	3	24	24	8	8	85	85	15	15	69	69	102	102
1 → 4	3	13	39	26	78	4	12	63	189	30	90	60	180	15	45	3	43	129	9	27	36	108	19	57	53	159	24	72	25	75	51	153
1 → 5	7	3	21	17	119	11	77	89	623	9	63	52	364	19	133	7	29	203	0	0	23	0	0	0	30	210	31	217	35	245	86	602
1 → 6	15	0	0	10	150	0	0	99	1485	50	750	17	255	0	0	15	68	1020	0	0	0	0	0	0	0	0	0	0	9	135	21	315
2 → 3	0	36	0	83	0	27	0	106	0	91	0	63	0	68	0	0	124	0	8	0	30	0	7	0	62	0	15	0	61	0	84	0
2 → 4	2	6	12	18	36	9	18	21	42	4	8	17	34	7	14	2	13	26	5	10	16	32	4	8	29	58	2	4	10	20	12	24
2 → 5	6	3	18	5	30	0	0	24	144	8	48	13	78	21	126	6	13	78	0	0	7	42	0	0	15	90	6	36	9	54	26	156
2 → 6	14	0	0	17	238	0	0	22	308	13	182	4	56	0	0	14	22	308	0	0	0	0	0	0	0	0	0	0	5	70	6	84
3 → 4	0	12	0	18	0	6	0	23	0	21	0	16	0	11	0	0	24	0	3	0	8	0	2	0	21	0	7	0	16	0	18	0
3 → 5	4	1	4	1	4	3	12	10	40	1	4	5	20	14	56	4	6	24	0	0	2	8	0	0	2	8	0	0	5	20	7	28
3 → 6	12	0	0	9	108	0	0	9	108	7	84	1	12	0	0	12	8	96	0	0	0	0	0	0	0	0	0	0	1	12	1	12
4 → 5	0	4	0	4	0	2	0	6	0	5	0	5	0	5	0	0	4	0	0	0	2	0	0	0	6	0	3	0	5	0	6	0
4 → 6	8	0	0	4	32	0	0	3	24	2	16	1	8	0	0	8	4	32	0	0	0	0	0	0	0	0	0	0	0	0	1	8
5 → 6	0	0	0	2	0	0	0	2	0	2	0	2	0	0	0	0	2	0	0	0	0	0	0	0	0	0	0	0	2	0	2	0
		Ha_t =		Ha_t =		Ha_t =		Ha_t =		Ha_t =		Ha_t =		Ha_t =				Ha_t =		Ha_t =		Ha_t =		Ha_t =		Ha_t =		Ha_t =		Ha_t =		Ha_t =	
		113		891		131		3057		1348		1058		421				2024		40		375		73		610		344		700		1484	
		Δa =		Δa =		Δa =		Δa =		Δa =		Δa =		Δa =				Δa =		Δa =		Δa =		Δa =		Δa =		Δa =		Δa =		Δa =	
		0.64		1.65		1.13		3.4		2.27		1.9		0.95				2.29		0.74		1.65		1.18		1.26		2.59		1.82		2.1	

density (Dd), drainage frequency (Df) and anticline's hinge spacing (Hs) are shown in Table 4. Data reveal that values of PAF are higher than 70% in basins 13, 8, and 4 (77.49%, 71.42% and 70.49% respectively). The values of PAF in basins 1, 9 and 11 are close to 50% implying that mentioned basins are less tilted. The Hs values range from 4.25 km (basin 4) to 15.34 km (basin 3).

The values of basin shape (Bs) vary greatly among basins. The low value of Bs in basins 1 and 9 (1.32 and 1.22 respectively) shows the relatively circular shape of mentioned basins. The highest value of Bs is associated with basin 4 where its length is 4.76 times longer than its maximum width. Basins 10, 8, 13, 11 and 5 have high values of Bs indicating elongated basins.

The basin length to mean width ratio (Bl/Bmw) is also low in basins 1 and 9 (1.56 and 1.37 respectively) demonstrating their circular shape. The high values of Bl/Bmw ratio in basins 4, 10, 8, 6 (8.29, 4.9, 4.71 and 4.15 respectively) show the higher length compared to mean width of mentioned basins. The Bl/Bmw ratio in other basins ranges from 2 to 4 implying the less elongated shapes.

Drainage density (Dd) of basins ranges from 2.57 (basin 7) to 4.5 (basin 14). The values of drainage frequency (Df) vary greatly among basins ranging from 2.09 (basin 7) to 8.87 (basin 14). Table 4 shows that basins with higher drainage density have higher drainage frequency.

The bifurcation ratio (Rb) of basins varies from 3.46 (basin 14) to 4.75 (basin 12). The R index value ranges from 0.43 (basin 1) to 1.48 (basin 11). The higher r values of basins 11, 4 and 8 (Table 4) reveal the higher hierarchical anomaly of streams in mentioned basins.

The Pearson's correlation coefficient (r) and probability at 0.01 and 0.05 levels for morphometric parameters are given in Table 5. There is strong positive correlation between Δa and PAF indexes ($r = 0.844$, $p < 0.01$). The Δa is also positively related to Bs ($r = 0.732$, $p < 0.01$) and to Bl/Bmw ($r = 0.775$, $p < 0.01$) indicating that the drainage anomaly of basins increases in elongated basins. The Δa parameter is also positively correlated to R index ($r = 0.517$, $p < 0.05$).

Although the spacing of anticlines (Hs) is inversely correlated to Δa, PAF, Bs, Bl/Bmw ratio, Dd and Df and R indexes, the strong correlations are associated with Hs–Δa ($r = -0.708$, $p < 0.01$), Hs–PAF ($r = -0.529$, $p < 0.05$) and Hs–Bs ($r = -0.516$, $p < 0.05$) pairs.

There are no meaningful correlations between Δa–Dd, and Δa–Df and Δa–Rb pairs (Table 5). A strong positive correlation exists between PAF and Bl/Bmw ratio ($r = 0.519$, $p < 0.05$) while there are no meaningful correlations between PAF–Dd, PAF–Df, PAF–Rb and PAF–R pairs. There are positive correlations between PAF and Bs as well as between PAF and R indexes with low r values (Table 5).

The Bs index is strongly related to Bl/Bmw ($r = 0.96$, $p < 0.01$) and to R index ($r = 0.659$, $p < 0.01$). The Bl/Bmw index is strongly correlated to R index ($r = 0.703$, $p < 0.01$). Although there is strong correlation between drainage density and drainage frequency ($r = 0.937$, $p < 0.01$), the Da and Df have no meaningful correlations with other parameters.

Overall data show the dependence of Δa index, as indicator of drainage system anomaly, on the PAF, Bs, Bl/Bmw, R and Hs indexes. Fig. 6 shows the linear regressions for Δa–PAF, Δa–Bs, Δa–Bl/Bmw and Δa–R pairs.

Above data show that more elongated and tilted basins have higher values of Δa and R indexes (see Tables 3 and 4) as indicators of hierarchical anomaly of drainage system.

6. Discussion

The deeply entrenched rivers (Fig. 2c, d), triangular facets with long bases (Fig. 8a) wine-glass valleys with narrow outlets (Fig. 2e), the presence of a wind gap and water gap (Fig. 2f) and the asymmetric forked drainage networks (Ramsey et al., 2008; Bretis et al., 2011; Bahrami, 2012, Fig. 4) are geomorphic indicators of active tectonics of Zagros anticlines. Although the Zagros Mountains are tectonically active, the rates of

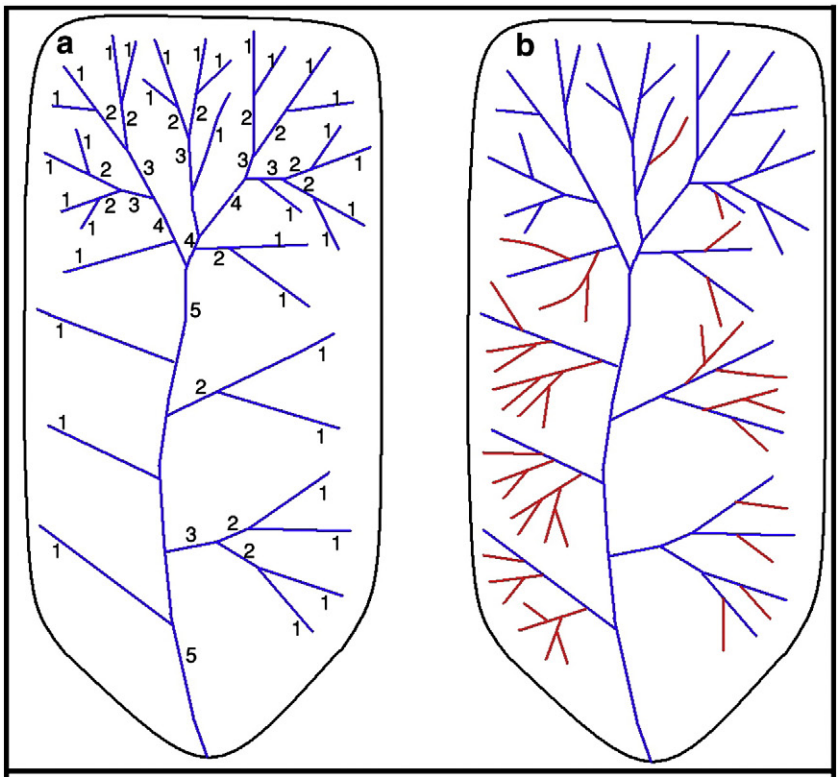

c

Anomalous stream junctions (i→j)	$Ha_{i\to j} = 2^{(j-2)} - 2^{(i-1)}$	$Ns_{i\to j}$	$(Ha_{i\to j} \times Ns_{i\to j})$
1→3	1	2	2
1→4	3	1	3
1→5	7	3	21
2→4	2	1	2
2→5	6	1	6
3→5	4	1	4

$\sum = 38$

$Ha_t = 38$

$N_1 = 34$

$\Delta a = Ha_t / N_1 = 38/34$

$\Delta a = 1.12$

Fig. 5. The procedure of calculation of $Ha_{i\to j}$, Ha_t and Δa parameters in a conceptual basin: (a) a conceptual 5th stream order basin with some anomalous stream junctions; (b) the manual hierarchical organization of drainage system of basin a, based on Avena et al. (1967) method; red streams are first-order drainages added manually to make the drainage network perfectly hierarchised; (c) The procedure for calculation of $Ha_{i\to j}$, Ha_t and Δa indexes introduced in this study.

uplift and shortening vary within different parts of Zagros Belt (Hessami et al., 2006; Nilforoushan et al., 2003; Vernant et al., 2004). The rate of uplift and tectonic activity can also vary locally within an anticline (Bahrami, 2012, 2013). Among geomorphic indexes, drainage systems are very sensitive to active tectonics especially to uplift of fold systems.

Although some studies imply that drainage network characteristics in the Zagros Mountains are affected by tectonic activity (Bahrami, 2012; Bretis et al., 2011; Piraste et al., 2011; Ramsey et al., 2008), this study focuses on the hierarchical anomaly of drainage systems and its relevance to active tectonics.

The Zagros folds vary in size and geometry, ranging from a few hundred meters to more than 10 km in wavelength and from a few kilometers to tens or even hundreds of kilometers in length (Sepehr et al., 2006). In addition, the rate of uplift and shortening vary greatly within Zagros Mountains (Vernant et al., 2004; Hessami et al., 2006). Above-mentioned variations in uplift, shortening and fold geometries have resulted in the variations of morphometric parameters of basins formed between folds. The folds variations also have considerable effects on the differences of drainage system pattern and anomaly. For example, in the long and narrow basins (i.e. basins 4 and 8) located between steep anticlines, parallel and trellis drainage patterns are developed that increase the hierarchical anomaly number and hence the Δa value. On the other hand, the dendritic drainage pattern has been formed in the relatively circular basins (1 and 9) decreasing the stream

Table 4
The values of percent of asymmetry factor (PAF), Basin shape (Bs), basin length to mean width ratio (Bl/Bmw), Drainage density (Dd), drainage frequency (Df), bifurcation ratio (Rb), bifurcation index (R) and anticline hinge spacing (Hs) of studied basins.

Basin no.	PAF	Bs	Bl/Bmw ratio	Dd	Df	Rb	R	Hs (km)
1	50.63	1.32	1.56	3.41	5.86	3.66	0.43	10.9
2	54.22	2.08	2.98	3.62	4.77	3.66	1.18	8.4
3	59.32	1.47	2.00	3.28	4.55	3.51	0.81	15.34
4	70.49	4.76	8.29	3.14	3.95	4.1	1.44	4.25
5	63.49	2.17	3.81	2.88	3.16	3.76	1.13	6.1
6	66.65	2.08	4.15	3.38	5.51	3.76	0.98	8.1
7	57.02	2.06	3.73	2.57	2.09	4.62	1.19	13.51
8	71.42	2.64	4.71	3.45	4.43	4.08	1.29	7.25
9	52.60	1.22	1.37	3.65	6.54	3.83	0.86	7.95
10	58.66	3.53	4.90	3.45	4.2	4.15	1.22	6.66
11	52.60	2.20	3.44	3.81	7.07	4.38	1.48	7.34
12	59.76	2.19	3.63	3.94	7.01	4.75	0.96	9.5
13	77.49	2.33	3.68	3.64	6.81	3.6	1.05	5.11
14	66.50	2.11	2.78	4.5	8.87	3.46	0.78	5.36
15	66.76	1.78	2.72	3.58	5.77	3.93	1.07	6.06

hierarchical anomaly. The basin shape control on drainages anomaly is validated by linear regressions for Bs–Δa and Bl/Bmw–Δa pairs revealing that the drainage anomaly of basins increases with increasing the length of basins (Fig. 6b, c).

The folding of Zagros belt become younger from northeast to southwest demonstrating that the deformation front is migrating from suture zone, in the northeast, towards the foredeep zone, in the southwest (Berberian, 1995). This is the case in the study area where structures around basins 1, 7, 9 and 12 in the southwestern part of Zagros are wider whereas structures around other basins in the northeast are tighter. This has resulted in the lower drainage hierarchical anomaly of basins 1, 7, 9 and 12 compared with other basins (see Δa, Table 3).

Results of this study also show that drainage anomaly of basins are also controlled by tilting of basins so that the Δa increases with increasing percent of basin asymmetry (Fig. 6a). As Colman-Sadd (1978) noted, most of the folds in the Simply Folded Belt are asymmetric and, with a few exceptions, the steepest limbs of the anticlines are on the southwest. Variation in the uplift rate of folds has resulted in the tilting of anticlinal basins. Evaluating the height of study area anticlines reveals that, in most cases, the northeastern anticlines are more uplifted (due to older age of anticlines) coinciding with the Berberian's (1995) study indicated that uplift is migrating from the suture zone (northeast) towards the southwest and hence the northeastern anticlines are older and more uplifted. Older and more uplifted northeastern anticlines cause the trunk river of basins migrates toward the southwest (younger anticlines). The migration of trunk river from high amplitude and older anticline toward younger anticlines of study area is shown schematically in Fig. 7. The movement of trunk river toward southwest is especially observed in basin 4 located between older and more uplifted Noakoh

Table 5
Pearson's correlation matrix for morphometric variables of studied basins.

	Δa	PAF	Bs	Bl/Bmw	Dd	Df	Rb	R	Hs
Δa	1								
PAF	0.844**	1							
Bs	0.732**	0.442	1						
Bl/Bmw	0.775**	0.519*	0.96**	1					
Dd	−0.067	0.044	−0.155	−0.28	1				
Df	−0.138	0.038	−0.291	−0.376	0.937**	1			
Rb	−0.143	−0.19	0.281	0.342	−0.218	−0.24	1		
R	0.517*	0.25	0.659**	0.703**	−0.241	−0.36	0.49	1	
Hs	−0.708**	−0.529*	−0.516*	−0.467	−0.364	−0.317	0.128	−0.384	1

** Significant correlation at the 0.01 level.
* Significant correlation at the 0.05 level.

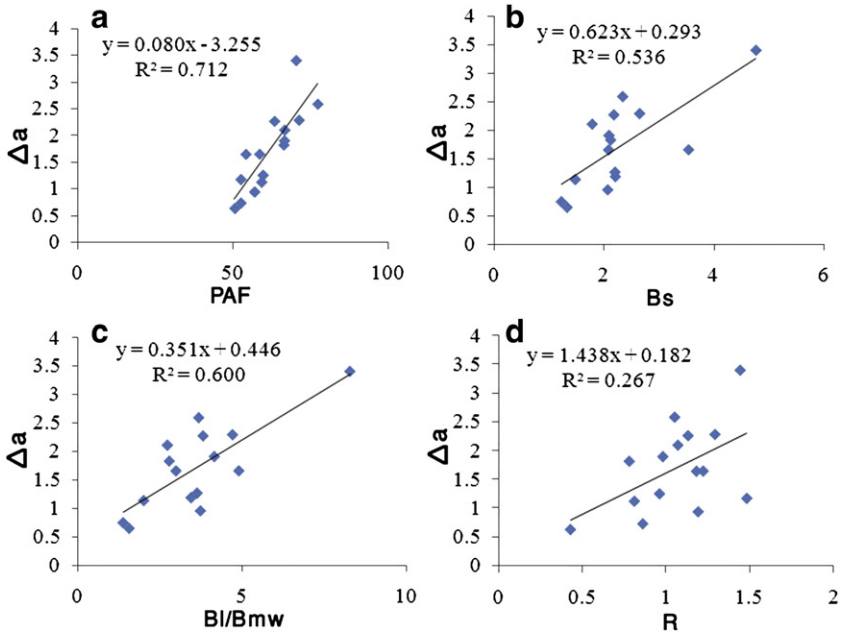

Fig. 6. Linear relationships and R^2 values between morphometric parameters of basins: (a) PAF versus Δa; (b) Bs versus Δa; (c) Bl/Bmw versus Δa; (d) R versus Δa.

anticline (in the northeast) and paykola anticline (in the southwest). The trunk river of basin 4 receives the first order streams of paykola anticline (Fig. 8). The higher rate of uplift in Noakoh anticline (Fig. 8a) compared to Paykola anticline (Fig. 8b) has resulted in the asymmetry of basin 4 and, hence, joining of the lower order streams, specially first order ones, to the higher order trunk river has increased the rate of Δa.

The trends of anticlines vary greatly within Zagros Mountains (Abdollahie Fard et al., 2006; Sherkati and Letouzey, 2004). The variations in trends and hinges of anticlines greatly control the shape of basins and thereby the hierarchical anomaly of drainages. In some cases, anticlines axes become closer to each other, in the downstream direction. On the other hand, some anticlines axes become closer to each other, in the upstream direction. The downward widening and narrowing of a basin due to the change in the trend of anticlines hinge is shown schematically in Fig. 9. Where the basin widens in the downstream direction (Fig. 9, basin A), the probability of joining of lower order stream to higher order streams (i.e. 1 → 5 or 1 → 6) is low and therefore the drainage's hierarchical anomaly (Δa) will be low (i.e. basins 7, 3 and 10). The mentioned basins can be considers as long triangular shape basins, being wider in the downstream direction.

Where the basin becomes narrower in the downstream direction (Fig. 9, basin B), the probability of joining of lower order stream to higher order streams is high (see plan view of basin B, Fig. 9) and therefore the Δa increases (i.e. basins 13, 5 and 8). The mentioned basins can be considered as pear shape basins, being narrower in the downstream direction.

Results show that most studied basins are synclinal basins located between anticlines. Only a few basins (1, 9 and 12) are erosional basins formed on the eroded anticlines. Basins 1, 9 and 12 have been developed on eroded parts of Emam-hasan, Saourghe and Kabir-Kuh anticlines

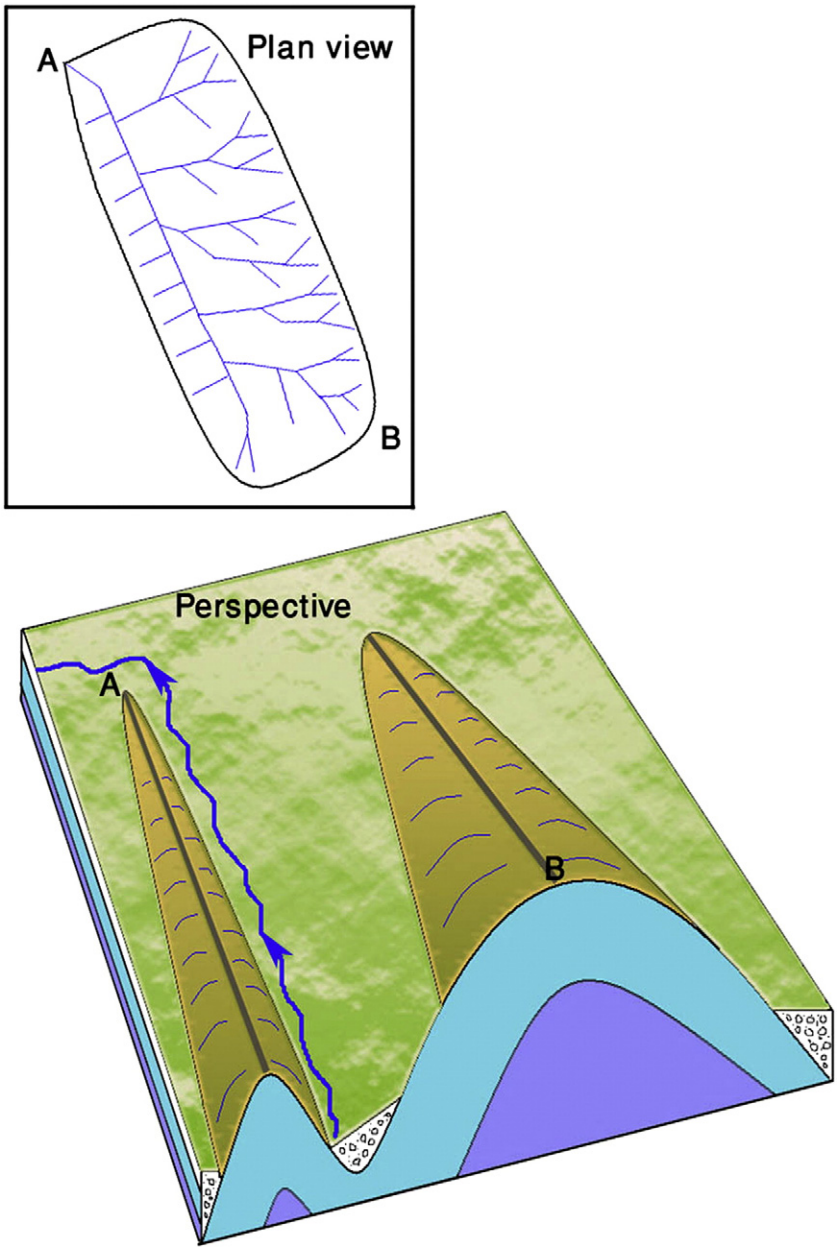

Fig. 7. The schematic representation of the effect of variation in uplift in basin tilting. The older northeastern anticlines are more uplifted, causing the movement of trunk river of basin toward the younger anticline in southwest and, hence, the joining of lower order streams (especially 1st order) of younger anticline to the higher order trunk river can increase the rate of Δa.

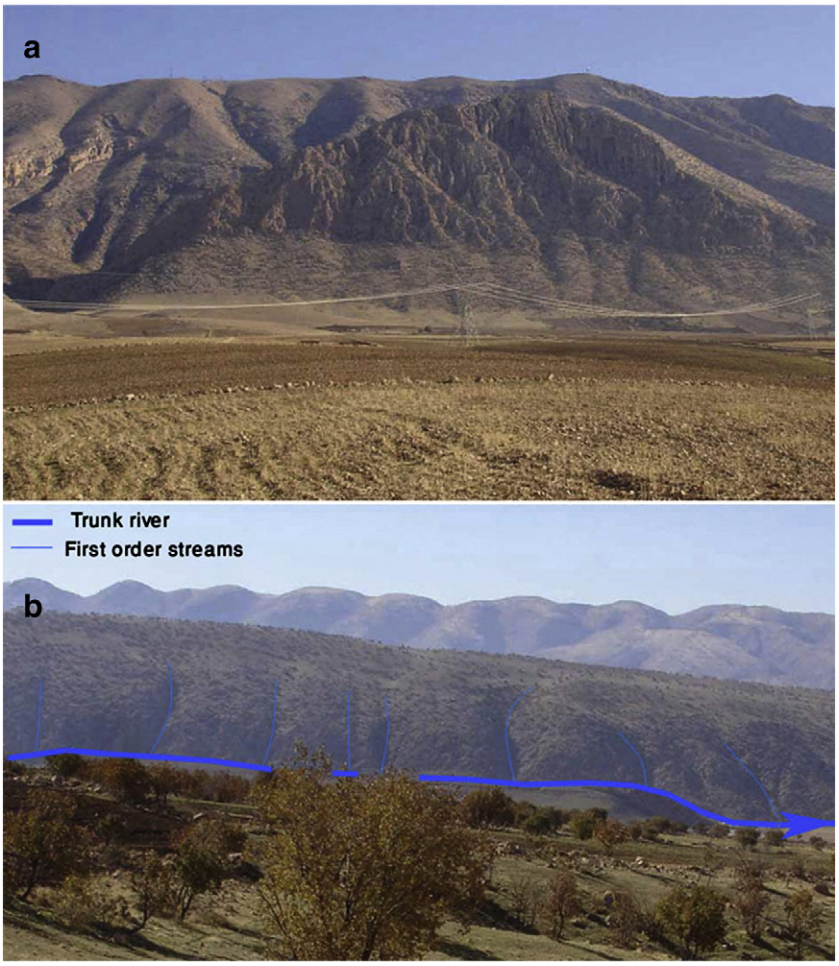

Fig. 8. The trunk river of basin 4 receives the first order streams of young paykola anticline. The higher rate of uplift of Noakoh anticline (a) has resulted in the asymmetry of basin 4 and in the movement of trunk river toward the Paykola anticline (b). The joining of first order streams to the higher order trunk river is obviously observed.

respectively. Data show that drainage anomaly is low in the erosional basins (Table 3) due to their circular shapes and dendritic drainage patterns. Fig. 10 shows schematically the higher drainage anomaly of long structural basins between linear anticlines and lower drainage anomaly of circular erosional basins.

It is worth noting that the rate of tectonic activity can be related to hinge spacing of anticline (Fig. 11) so that tectonically active parts of Zagros (i.e. northeast) is characterized by the tight and short-wavelength folds. Fig 11 clearly displays that anticline's hinge spacing increases from northeast toward southwest. It means that the structures (anticlines and synclines) in the northeast are tighter and older while the structures in the southwest are younger and wider (less compressed), according with Verges et al. (2011) implying that amounts of shortening of Zagros folds decrease from northeast (Pusht-e Kuh arc) toward southwest (Dezful embayment).

As Table 5 shows, the hinge spacing of anticlines strongly controls the Δa, PAF and Bs indexes. The three mentioned parameters increase with decreasing hinge spacing implying that areas with lower hinge spacing of anticlines are characterized by higher values of Δa, PAF and Bs indexes.

For a better understanding of the effect of anticline hinge spacing on the Δa index, the basins can be categorized into two groups (A and B). Basins of group A (1, 7, 8, 9, 10, 11 and 12) are located in the southwestern part of Zagros whereas basins of group B (2, 3, 4, 5, 6, 13, 14, and 15) are located in the northeastern domain of Zagros (Fig. 1). The mean of Δa index in basins of group A is 1.24 while it is 2.11 in those of group B. The mean of Hs index in basins of group A is 9.02 km whereas it is 7.34 km in basins of group B. Hence, the hinge spacing as a representative of tectonic activity strongly controls the hierarchical anomaly of drainage, the basin tilting and shape. Data reveal that the Δa index of basins does not depend on the drainage density and frequency as well as on bifurcation ratio. The variations in the values of drainage density and frequency and bifurcation ratio and the low R^2 values between Δa–Dd, Δa–Df and Δa–Rb pairs can be attributed to the differences in basins lithology (Table 2).

Although Carbonate karstic formations outcrop in about 23% of the Zagros mountains (Ashjari and Raeisi, 2006), there are significant variations in the area of mentioned formations among studied basins. Asmari and Saravk formations form productive groundwater aquifers feeding karstic springs in Zagros region (Hajikazemi et al., 2010; Karimi et al., 2005). Asmari and Saravk are the most permeable formations and have large capacity to infiltrate the overland flow and, thus, to decrease drainage density and frequency of basins. In contrast, Gachsaran, Agha Jari, Pabdeh, Gurpi are impermeable formations (Karimi et al., 2005; Raeisi and Karimi, 1997) that can result in higher drainage density and frequency. Quaternary Alluvium is relatively permeable formation that has relatively good capacity to decrease drainage density.

As Table 1 shows, drainage density is higher in basins in which the area of Asmari, Saravk and Quaternary alluvium formations is higher. For example, the highest value of drainage density and frequency is associated with basin 14 in which the area percent of permeable formations (Asmari, Sarvak and alluvium) is low. The least value of Dd and Df is related to basin 7 (Table 1) in which the permeable Asmari and alluvium formations comprise 68.2% and 33.9% of basin area respectively. Overall, basins that are dominantly covered by permeable formations (i.e. basins 4, 5, 6, 7) have higher drainage density and frequency.

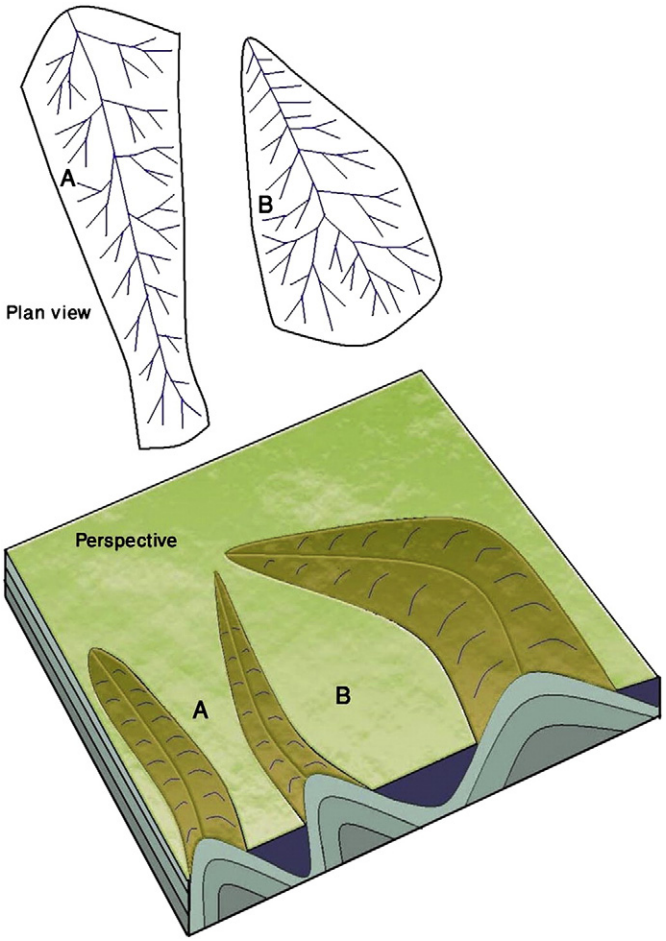

Fig. 9. The schematic representation of the effect of variation in anticline trend on the basin shape. Where the anticlines axes diverge in the downstream direction, the basin widens downward. As a result, long triangular shape basins is formed being wider in the downstream direction (see plan view of basin A). In this case, the probability of joining of lower order streams to higher order streams is low and therefore the drainage's hierarchical anomaly decreases. Where the anticlines axes become closer to each other, in the downstream direction, the basin becomes narrower downward. Therefore, the pear shape basins, being narrower downward, are developed (see plan view of basin B). In this case, the probability of joining of lower order streams to higher order streams is high and therefore the Δa will be high.

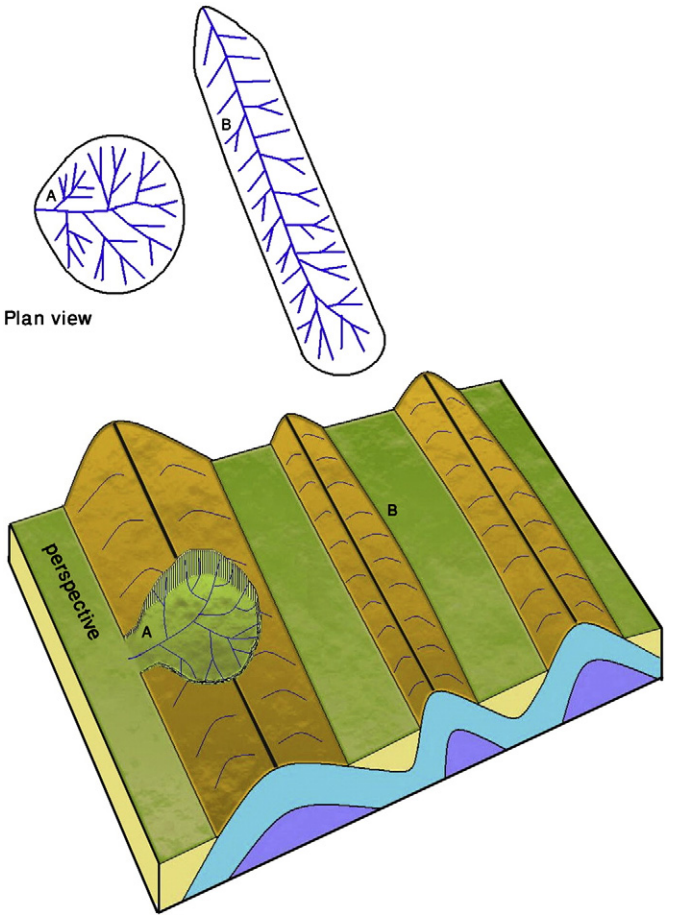

Fig. 10. Schematic comparison of the effect of structural and erosional basins on drainage anomaly. The elongated structural basin (B) located between linear anticlines have higher rates of Δa, due to the joining of lower order streams to the trunk stream. The erosional basin (A) formed on the eroded anticline is nearly circular having dendritic drainage pattern with lower Δa.

7. Conclusion

1. The morphometric analysis of hierarchical organization of drainage networks plays an important role in understanding the tectonic effects on basins development. This study, for the first time, introduced equations for calculation of hierarchical anomaly number to compute quantitatively the drainage hierarchical anomaly index (Δa) for 15 basins in Zagros Folded Belt.
2. Since the rate of tectonic activity varies within different parts of Zagros, 15 basins were selected in different parts of folded belt of Zagros. The statistical relations between drainage system indexes (Δa, R, Rb, Dd and Df), indexes of basin morphometry (PAF, Bl and Bl/Bmw) and hinge spacing of anticlines were analyzed.
3. Results show that Δa is strongly correlated with PAF, Bs, Bl/Bmw and R indexes. The variations in trend of anticlines greatly control the shape of basins. Where anticlines hinges become closer to each other in the downstream direction (known as pear shape basins in this study), basin become narrower downward and hence the Δa increases due to the joining of lower order stream to higher order streams.
4. The tilting of basins is controlled by variation in the rate of uplift of anticlines so that older and more uplifted northeastern anticlines cause the trunk river of basins migrate toward the younger anticlines in southwest and hence Δa increases, as trunk river of basin (having high order) receives a lot of first order streams of younger anticline.
5. Results also reveal that elongated structural basins located between linear anticlines have higher rates of Δa, compared with nearly circular shape/erosional basins formed on the eroded anticlines.
6. Since the intensity of tectonic activity and deformation of Zagros folds decrease from northeast toward southwest, the hinge spacing of anticlines increases southwestwards. Results show that the Hs index strongly controls the basin's shape and tilting and hence hierarchical anomaly of drainages so that Δa decreases with increasing Hs index.
7. Overall, the drainage network anomaly is strongly controlled by basin's tilting and shape so that basins that have been greatly elongated and tilted have the highest values of Δa.
8. As the elongation (shape) and tilting of basins are controlled by variation in the rates of folding, uplift and hinge spacing and by the trend of anticlines, it can be concluded that the hierarchical anomaly of drainage systems of studied basins are controlled by tectonic activities.

Acknowledgments

Financial support from the Hakim Sabzevari University is greatly appreciated. The author is grateful to unknown reviewers for their

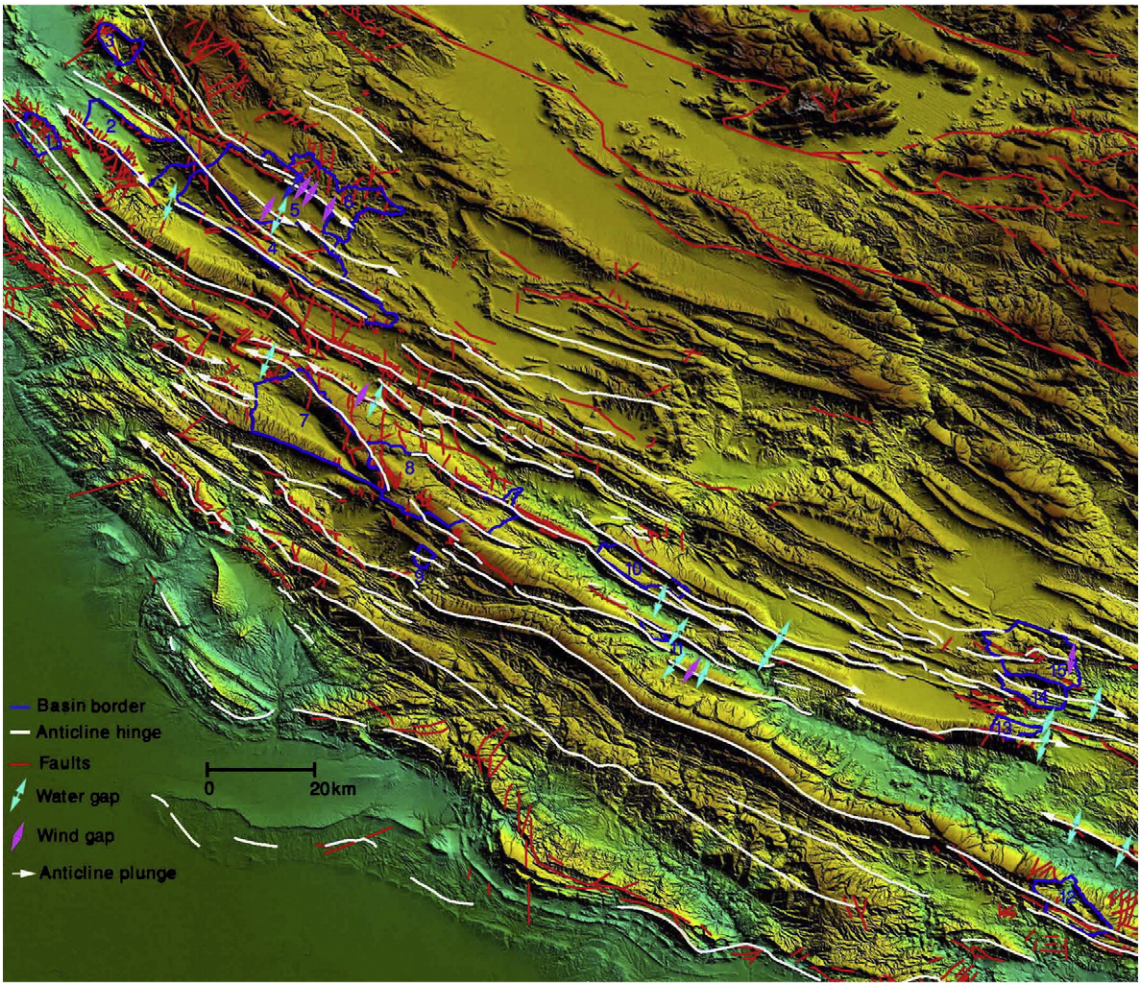

Fig. 11. Anticline hinges (axial traces), faults, water gaps, wind gaps, anticline plunges of study area and borders of studied basins. Towards the northeast, anticline's hinge spacing decrease due to the increase in the intensity of deformation and tectonic activity. For example, hinge spacing is more in basins 1, 7, 9 and 12 than other ones.

constructive suggestions for improvement of the earlier versions of the manuscript.

References

Abdollahie Fard, I., Braathen, A., Mokhtari, M., Alavi, S.A., 2006. Interaction of the Zagros Fold–Thrust Belt and the Arabian-type, deep-seated folds in the Abadan Plain and the Dezful Embayment, SW Iran. Petroleum Geoscience 12, 347–362.

Abrahams, A.D., 1984. Channel networks: a geomorphological perspective. Water Resources Research 20, 161–188.

Alavi, M., 2004. Regional stratigraphy of the Zagros fold–thrust belt of Iran and its proforeland evolution. American Journal of Science 304, 1–20.

Alipoor, R., Poorkermani, M., Zare, M., El Hamdouni, R., 2011. Active tectonic assessment around Rudbar Lorestan dam site, High Zagros Belt (SW of Iran). Geomorphology 128, 1–14.

Alipoor, R., Zaré, M., Ghassemi, M.R., 2012. Inception of activity and slip rate on the Main Recent Fault of Zagros Mountains, Iran. Geomorphology 175, 86–97.

Altin, T.b, Altin, B.N., 2011. Development and morphometry of drainage network in volcanic terrain, CentralAnatolia, Turkey. Geomorphology 125, 485–503.

Ashjari, J., Raeisi, E., 2006. Influences of anticlinal structures on regional flow, Zagros Iran. Journal of Cave and Karst Studies 68, 118–129.

Avena, G.C., Giuliano, G., Lupia Palmieri, E., 1967. Sulla valutazione quantitativa della gerarchizzazione ed evoluzione dei reticoli fluviali. Bollettino della Societa Geologica Italiana 86, 81–796.

Bahrami, S., 2012. Morphotectonic evolution of triangular facets and wine-glass valleys in the Noakoh anticline, Zagros, Iran: implications for active tectonics. Geomorphology 159, 37–49.

Bahrami, S., 2013. Tectonic controls on the morphometry of alluvial fans around Danehkhoshk anticline, Zagros, Iran. Geomorphology 180–181, 217–230.

Berberian, M., 1995. Master 'blind' thrust faults hidden under the Zagros folds: active basement tectonics and surface morphotetonics. Tectonophysics 241, 193–224.

Berberian, M., King, G.C.P., 1981. Towards a paleogeography and tectonic evolution of Iran. Canadian Journal of Earth Sciences 18, 210–265.

Blanc, E.J.P., Allen, M.B., Inger, S., Hassani, H., 2003. Structural styles in the Zagros Simple Folded Zone, Iran. Journal of the Geological Society of London 160, 401–412.

Bretis, B., Bartl, N., Grasemann, B., 2011. Lateral fold growth and linkage in the Zagros fold and thrust belt (Kurdistan, NE Iraq). Basin Research 23, 615–630.

Bull, W.B., McFadden, L.D., 1977. Tectonic geomorphology north and south of the Garlock fault, California: in Geomorphology in Arid Regions. In: Doehring, D.O. (Ed.), Proceedings 8th Annual Geomorphology Symposium, State University New York at Binghamton, pp. 115–137.

Burbank, D.W., Anderson, R.S., 2001. Tectonic Geomorphology. Blackwell Science, Oxford (274 pp.).

Burberry, C.M., Cosgrove, J.W., Liu, J.G., 2010. A study of fold characteristics and deformation style using the evolution of the land surface: Zagros Simply Folded Belt, Iran. Geological Society, London Special Publication 330, 139–154.

Cannon, P.J., 1976. Generation of explicit parameters for a quantitative geomorphic study of Mill Creek drainage basin. Oklahoma Geology Notes 36, 3–16.

Casciello, E., Vergés, J., Saura, E., Casini, G., Fernández, N., Blanc, E., Homke, S., Hunt, D.W., 2009. Fold patterns and multilayer rheology of the Lurestan Province, Zagros Simply Folded Belt (Iran). Journal of the Geological Society 166, 947–959.

Ciccacci, S., Fredi, P., Lupia Palmieri, E., Pugliese, F., 1986. Indirect evaluation of erosion entity in drainage basins through geomorphic, climatic and hydrological parameters. In: Gardiner, V. (Ed.), International Geomorphology Part 2. John Wiley & Sons Ltd, Chichester, pp. 33–48.

Colman-Sadd, S.P., 1978. Fold development in Zagros simply folded belt, southwest Iran. AAPG 62, 984–1003.

Deffontaines, B., Chorowicz, J., 1991. Principles of drainage basin analysis from multisource data: application to the structural analysis of the Zaire Basin. Tectonophysics 194, 237–263.

Deffontaines, B., Chotin, P., Air Brahim, L., Rozanov, M., 1992. Investigation of active faults in Morocco using morphometric methods and drainage pattern analysis. Geologische Rundschau 81, 199–210.

Delcaillau, B., Deffontaines, B., Floissac, L., Angelier, J., Deramond, J., Souquet, P., Chu, H.T., Lee, J.F., 1998. Morphotectonic evidence from lateral propagation of active frontal fold; Pakuashan anticline, foothills of Taiwan. Geomorphology 24, 263–290.

Delcaillau, B., Carozza, J.M., Laville, E., 2006. Recent fold growth and drainage development, the Janauri and Chandigarh Anticlines in the Siwalik Foothills, Northwest India. Geomorphology 76, 241–256.
Della Seta, M., Del Monte, M., Fredi, P., Lupia Palmieri, E., 2009. Space–time variability of denudation rates at the catchment and hillslope scales on the Tyrrhenian side of Central Italy. Geomorphology 107, 161–177.
Della, Seta M., Del Monte, M., Fredi, P., Lupia Palmieri, E., 2007. Direct and indirect evaluation of denudation rates in Central Italy. Catena 71, 21–30.
Devi, R.K.M., Bhakuni, Bora, P.B., 2011. Tectonic implication of drainage set-up in the Sub-Himalaya: a case study of Papumpare district, Arunachal Himalaya, India. Geomorphology 127, 14–31.
El Hamdouni, R., Irigaray, C., Fern ndez, T., Chac n, J., Keller, E.A., 2008. Assessment of relative active tectonics, southwest border of the Sierra Nevada (Southern Spain). Geomorphology 96, 150–173.
Emami, H., 2008. Foreland Propagation of Folding and Structure of the Mountain Front Flexure in the Pusht-EKuh Arc (Zagros, Iran). (Ph.D Thesis) Universitat de Barcelona, Barcelona.
Faghih, A., Samani, B., Kusky, T., Khabazi, S., Roshanak, R., 2012. Geomorphologic assessment of relative tectonic activity in the Maharlou Lake Basin, Zagros Mountains of Iran. Geological Journal 47, 30–40.
Falcon, N.L., 1969. Problems of the relationship between surface structure and deep displacements illustrated by the Zagros Range. In: Kent, P.E., Satterthwaite, G.E., Spencer, A.M. (Eds.), Time and place in orogeny: London. Geological Society Special Publication, 3, pp. 9–22.
Falcon, N.L., 1974. Southern Iran: Zagros Mountains. In: Spencer, A.M. (Ed.), Mesozoic–Cenozoic Orogenic Belts. Data for Orogenic Studies: Geological Society of London, Special Publication, vol. 4, pp. 199–211.
Giaconia, F., Booth-Rea, G., Martínez-Martínez, J.M., Azañón, J.M., Pérez-Peña, J.V., 2012. Geomorphic analysis of the Sierra Cabrera, an active pop-up in the constructional domain of conjugate strike-slip faults: the Palomares and Polopos fault zones (eastern Betics, SE Spain). Tectonophysics 580, 27–42.
Gioia, D., Martino, C., Schiattarella, M., 2011. Long- to short-term denudation rates in the southern Apennines: geomorphological markers and chronological constraints. Geologica Carpathica 62, 27–41.
Grauso, S., Fattoruso, G., Crocetti, C., Montanari, A., 2008. Estimating the suspended sediment yield in a river network by means og geomorphic parameters and regression relationships. Hydrology and Earth System Sciences 12, 177–191.
Guarnieri, P., Pirrotta, C., 2008. The response of drainage basins to the late Quaternary tectonics in the Sicilian side of the Messina Strait (NE Sicily). Geomorphology 95, 260–273.
Hajikazemi, E., Al-Aasm, I.S., Coniglio, M., 2010. Subaerial exposure and meteoric diagenesis of the Cenomanian-Turonian Upper Sarvak Formation, southwestern Iran. Geological Society, London, Special Publications 330, 253–272.
Han, Z., Wu, L., Ran, Y., Ye, Y., 2003. the concealed active tectonics and their characteristics as revealed by drainage density in the North China Plain (NCP). Journal of Asian Earth Sciences 21, 989–998.
Hessami, K., Nilforoushan, F., Talbot, C.J., 2006. Active deformation within the Zagros Mountains deduced from GPS measurements. Journal of the Geological Society of London 163, 143–148.
Horton, R.E., 1932. Drainage basin characteristics. Transactions, AmericanGeophysical Union 13, 350–361.
Horton, R.E., 1945. Erosional development of streams and their drainage basins; hydrophysical approach to quantitative morphology. Geological Society of America Bulletin 56 (3), 275–370.
Jackson, J., Van Dissen, R., Berryman, K., 1998. Tilting of active folds and faults in the Manawatu region, New Zealand: evidence from surface drainage patterns, New Zealand. Journal of Geology and Geophysics 41, 377–385.
Jamieson, S.S.R., Sinclair, H.D., Kirstein, L.A., Purves, R.S., 2004. Tectonic forcing of longitudinal valleys in the Himalaya, morphological analysis of the Ladakh batholith. North India, Geomorphology 58, 49–65.
Karimi, H., Raeisi, E., Bakalowicz, M., 2005. Characterising the main karst aquifers of the Alvand basin, Northwest of Zagros, Iran, by a hydrogeochemical approach. Hydrogeology Journal 13, 787–799.
Keller, E.A., Pinter, N., 2002. Active tectonics: earthquakes, uplift, and landscape (second edition): Englewood Cliffs. Prentice Hall, New Jersey (362 pp.).
Keller, E.A., Gurrola, L.D., Tierney, T.E., 1999. Geomorphic criteria to determine direction of lateral propagation of reverse faulting and folding. Geology 27, 515–518.
Krishnamurthy, J., Srinivas, G., Jayaram, V., Chandrasekhar, M.G., 1996. Influence of rock types and structures in the development of drainage networks in typical hardrock terrain. ITC J. 3–4, 252–259.
Kumar, R., Kumar, S., Lohani, A.K., Nema, R.K., Singh, R.D., 2000. Evaluation of geomorphological characteristics of a catchment using GIS. GIS India 9, 13–17.
Lawa, F.A., Koyi, H., Ibrahim, A., 2013. Tectono-stratigraphic evolution of the NW segment of the Zagros Fold–Thrust belt, Kurdistan, NE Iraq. Journal of Petroleum Geology 36, 75–96.
Leopold, L.B., Miller, J.P., 1956. Ephemeral streams: hydraulic factors and their relation to the drainage network. U.S. Geological Survey, professional paper 282-A.
Melosh, B.L., Keller, E.A., 2013. Effects of active folding and reverse faulting on stream channel evolution, Santa Barbara Fold Belt, California. Geomorphology 186, 119–135.
Nilforoushan, F., Vernant, P., Masson, F., et al., 2003. GPS Network Monitors the Arabia–Eurasia Collision Deformation in Iran. Journal of Geodesy 77, 411–422.
Ozdemir, H., Bird, D., 2009. Evaluation of morphometric parameters of drainage networks derived from topographic maps and DEM in point of floods. Environmental Geology 56, 1405–1415.
Ozkaymak, Ç., Sozbilir, H., 2012. Tectonic geomorphology of the Spildağı High Ranges, western Anatolia. Geomorphology 173, 128–140.
Piraste, S., Pradhan, B., Rizvi, S.M., 2011. Tectonic process analysis in Zagros Mountain with the aid of drainage networks and topography maps dated 1950–2001 in GIS. Arabian Journal of Geoscience 4, 171–180.
Raeisi, E., Karimi, G., 1997. Hydrochemographs of Berghan karst spring as indicators of aquifer characteristics. Journal of Cave and Karst Studies 59, 112–118.
Raj, R., 2012. Active tectonics of NE Gujarat (India) by morphometric and morphostructural studies of Vatrak River basin. Journal of Asian Earth Sciences 50, 66–78.
Ramasamy, S.M., Kumanan, C.J., Selvakumar, R., Saravanavel, J., 2011. Remote sensing revealed drainage anomalies and related tectonics of South India. Tectonophysics 501, 41–51.
Ramírez-Herrera, M.T., 1998. Geomorphic assessment of active tectonics in the Acambay Graben, Mexican volcanic belt. Earth Surface Processes and Landforms 23, 317–332.
Ramsey, L.A., Walker, R.T., Jackson, J., 2008. Fold evolution and drainage development in the Zagros mountains of Fars province, SE Iran. Basin Research 20, 23–48.
Reddy, G.P.O., Maji, A.K., Gajbhiye, K.S., 2004. Drainage morphometry and its influence on landform characteristics in a basaltic terrain, Central India — a remote sensing and GIS approach. International Journal of Applied Earth Observation and Geoinformation 6, 1–16.
Schumm, S.A., 1997. Drainage density: problems of prediction'. In: Stoddart, D.R. (Ed.), Process and Form in Geomorphology, Routledge, London, pp. 15–45.
Sepehr, M., Cosgrove, J.W., Moieni, M., 2006. The impact of cover rock rheology on the style of folding in the Zagros Fold–thrust Belt. Tectonophysics 427, 265–281.
Shaban, A., Khawlie, M., Abdallah, C., Awad, M., 2005. Hydrological and watershed characteristics of the El-Kabir River, North Lebanon. Lakes & Reservoirs: Research & Management 10, 93–101.
Sherkati, S., Letouzey, J., 2004. Variation of structural style and basin evolution in the central Zagros (Izeh zone and Dezful Embayment). Iran, Marine and Petroleum Geology 21, 535–554.
Shreve, R.L., 1966. Statistical law of stream numbers. Journal of Geology 74, 17–37.
Simoni, A., Elmi, C., Picotti, V., 2003. Late Quaternary uplift and valley evolution in the Northern Apennines. Lamone Catchment, Quaternary International 101–102, 253–267.
Stocklin, J., 1968. Structural history and tectonics of Iran; a review. American Association of Petroleum Geologists Bulletin 52, 1229–1258.
Strahler, A.N., 1952. Hypsometric (area-altitude) analysis of erosional topography. Geological Society of America Bulletin 63, 1117–1142.
Strahler, A.N., 1957. Quantitative analysis of watershed geomorphology. Transactions, American Geophysical Union 38, 913–920.
Sung, O., Chen, Y.C., 2004. Geomorphic evidence and kinematic model for quaternary transfer faulting of the Pakuashan anticline, central Taiwan. Journal of Asian Earth Sciences 24, 389–404.
Talling, P.J., Sowter, M.J., 1999. Drainage density on progressively tilted surfaces with different gradients, Wheeler Ridge, California. Earth Surface Processes and Landforms 24, 809–824.
Tatar, M., Hatzfeld, D., Martinod, J., Walpersdorf, A., Ghafori-Ashtiany, M., Chéry, J., 2002. The present-day deformation of the central Zagros from GPS measurements. Geophysical Research Letters 29. http://dx.doi.org/10:1029/2002/GL015427.
Verges, J., Goodarzi, M.G.H., Emami, H., Karpuz, R., Efstathiou, J., Gillespie, P., 2011. Multiple detachment folding in Pusht-e Kuh arc, Zagros: role of mechanical stratigraphy. In: McClay, K., Shaw, J.H., Suppe, J. (Eds.), Thrust Fault-Related Folding: AAPG Memoir, 94, pp. 69–94.
Vernant, P., Nilforoushan, F., Hatzfeld, D., et al., 2004. Present-day Crustal Deformation and Plate Kinematics in Middle East Constrained by GPS Measurements in Iran and Northern Oman. Geophysical Journal International 157, 381–398.
Walker, F., Allen, M.B., 2012. Offset rivers, drainage spacing and the record of strike-slip faulting: the Kuh Banan Fault, Iran. Tectonophysics 530, 251–263.
Zhang, H.P., Liu, S.F., Yang, N., Zhang, Y.Q., Zhang, G.W., 2006. Geomorphic characteristics of the Minjiang Drainage Basin (Eastern Tibetan Plateau) and its Tectonic implications: new insights from a digital elevation model study. Island Arc 15, 239–250.